Testing nonunitarity of neutrino mixing matrices at neutrino factories

Srubabati Goswami[1,*] and Toshihiko Ota[2,+]

[1]*Harish-Chandra Research Institute, Chhatnag Road, Jhunsi, Allahabad 211 019, India*

[2]*Institut für Theoretische Physik und Astrophysik Universität Würzburg, Am Hubland 97074 Würzburg, Germany*

(Received 18 February 2008; published 21 August 2008)

In this paper we explore the effect of nonunitary neutrino mixing on neutrino oscillation probabilities both in vacuum and matter. In particular, we consider the $\nu_\mu \to \nu_\tau$ channel and, using a neutrino factory as the source for ν_μ's, discuss the constraints that can be obtained on the moduli and phases of the parameters characterizing the violation of unitarity. We point out how the new *CP* violation phases present in the case where the nonunitary mixings give rise to spurious "degenerate" solutions in the parameter space. We also discuss how the true solutions can be extricated by combining measurements at several baselines.

DOI: 10.1103/PhysRevD.78.033012 PACS numbers: 14.60.St, 13.15.+g, 14.60.Pq

I. INTRODUCTION

There is a phenomenal increase in our knowledge of neutrino properties in the past few years coming from neutrino oscillation data from solar, atmospheric, accelerator and reactor neutrino experiments. For three neutrino flavors, there are nine parameters characterizing the light neutrino mass matrix: the three masses, three mixing angles and three *CP* phases. Neutrino oscillation data determine the best-fit values and the 3σ ranges of the mass squared differences and mixing angles as [1]

(i) Combined analysis of solar and KamLAND reactor neutrino data gives the best-fit values and 3σ ranges of mass and mixing parameters as $\Delta m^2_{21} \equiv m^2_2 - m^2_1 = 7.9^{+1.0}_{-0.8} \cdot 10^{-5}$ eV^2 and $\sin^2\theta_{12} = 0.31^{+0.09}_{-0.08}$. The solar data imply $\Delta m^2_{21} > 0$.

(ii) Global analysis of atmospheric neutrino data from SuperKamiokande and data from accelerator experiments K2K and MINOS gives $|\Delta m^2_{31}| \equiv |m^2_3 - m^2_1| = 2.5^{+0.7}_{-0.6} \cdot 10^{-3}$ eV^2 and $\sin^2\theta_{23} = 0.5^{+0.38}_{-0.16}$.

(iii) The value of the third leptonic mixing angle θ_{13} is not yet known and at present it is bounded to be $\sin^2\theta_{13} < 0.05$, leaving open the possibility of very small or zero value for this.

This tremendous progress has initiated the precision era of neutrino physics, and experiments are planned and proposed to further increase the precision of the known neutrino parameters and to pin down the value of the mixing angle θ_{13} and determine the sign of Δm^2_{31} (sign$[\Delta m^2_{31}]$).[1]

A nonzero value of θ_{13} is intimately related to the possibility of observation of the *CP* phase in the lepton sector. A large value of θ_{13} would also enable one to determine the sign$[\Delta m^2_{31}]$ through observation of large matter effects for neutrinos propagating through Earth [2–5]. If θ_{13} is relatively large, $\sin^2 2\theta_{13} \gtrsim 0.01$, then the answers to these questions may be obtained from superbeam [6,7] and future atmospheric neutrino experiments [3,4,8–12]. However, if nature selects θ_{13} to be smaller than this, then one has to go to either β-beam or neutrino factory experiments. The R&D for both are actively pursued [13,14]. Future facilities also have the potential to discover new physics [15–20].

The best-fit values of masses and mixing angles quoted above are obtained assuming the neutrino mixing matrix [Pontecorvo-Maki-Nakagawa-Sakata (PMNS) matrix] to be unitary. However, for models with heavy fermionic fields, the deviation of the leptonic mixing matrix from unitarity is a generic feature [21–23]. A typical example is the type-I seesaw mechanism [24–30] which provides a natural framework of generating small neutrino masses. This requires introduction of one or more heavy right-handed singlet neutrino field(s). Although the full mixing matrix at the high scale is expected to be unitary in these cases, the mixing matrix relevant for low energy phenomenology is not unitary as the production of the heavy particles are kinematically forbidden. However, the violation from unitarity in the canonical type-I seesaw mechanism is found to be very small if the mass scale of the heavy neutrinos are of the order of the grand unified theory scale $\sim 10^{16}$ GeV and the heavy neutrinos decouple and do not influence the physics at low scale. However, nonminimal seesaw models have been constructed with heavy neutrinos of mass $\mathcal{O}(1)$ TeV, invoking symmetry arguments to suppress the seesaw term [31–34]. Such models can give rise to significant light-heavy mixing and deviation from unitarity. The TeV scale seesaw models are interesting as these can have signatures in the LHC in the near future [35–37]. Also successful leptogenesis can be generated if the heavy

*sruba@mri.ernet.in

+Toshihiko.Ota@physik.uni-wuerzburg.de

[1]Usually $\Delta m^2_{31} > 0$ and $m^2_3 \simeq \Delta m^2_{31} \gg m^2_2 \simeq \Delta m^2_{21} \gg m^2_1$ is referred to as normal hierarchy (NH), and $\Delta m^2_{31} < 0$ and $m^2_2 \simeq |\Delta m^2_{31}| + \Delta m^2_{21} > m^2_1 \simeq |\Delta m^2_{31}| \gg m^2_3$ as inverted hierarchy (IH). The three neutrinos can also be quasidegenerate with $m^2_3 \simeq m^2_2 \simeq m^2_1 \equiv m^2_0 \gg |\Delta m^2_{31}|$ in which there is no hierarchy. However, one can still ask what the sign of Δm^2_{31} is.

Majorana neutrinos are quasidegenerate [38–40]. There are also models with heavy neutral (gauge singlets) which can give large light-heavy mixings [41–43]. In the R-parity violating supersymmetric models, neutrinos can also mix with neutralinos [44]. The mixing between Kaluza-Klein modes of right-handed neutrinos in bulk space and active neutrinos can also induce the nonunitary PMNS matrix [45]. Since deviation from unitarity is due to the physics at the high scale, a measurement of these at the low scale can serve as a window to the physics at high energy. Hence it is important to probe if the future precision neutrino experiments can give any indication toward the nonunitary nature of the neutrino mixing matrix. In this paper we address this question.

The nonunitary nature of the neutrino mixing matrix due to mixing with fields heavier than $M_Z/2$ can manifest itself in tree level processes like $\pi \to \mu\nu$, $Z \to \bar{\nu}\nu$, $W \to l\nu$ or in flavor violating rare charged lepton decays like $\mu \to e\gamma$, $\tau \to \mu\gamma$, etc., which proceed via one-loop processes and hence can be constrained from low energy electroweak data [21,22,42,43,46–51]. Nonunitarity of neutrino mixing matrices can also affect the neutrino oscillation probabilities [52–58]. In this paper, we concentrate on the effect of nonunitarity on neutrino oscillation probabilities and the possibility of probing this in neutrino factories. We show that the effect of nonunitarity can be more pronounced in the appearance channel than in the survival channel. In particular, we look into the effect of deviation from nonunitarity in the $\nu_\mu - \nu_\tau$ channel since the present constraint on the nonunitarity parameter in this channel is much weaker than the constraint on the $\nu_e - \nu_\mu$ channel. We consider ν_τ detectors like the OPERA [59] or ICARUS [60] detectors for CERN to Gran Sasso $\nu_\mu \to \nu_\tau$ oscillation search program and discuss the possibility of constraining the moduli and phases parametrizing the unitarity violation. These phases characterizing the nonunitarity constitute a new source for CP violation which can be present even in the limit of $\theta_{13} \to 0$. We also discuss the matter effects in the presence of nonunitarity and show that for a nonunitary mixing matrix, matter effect can manifest itself even in the limit of the third leptonic mixing angle $\theta_{13} \to 0$ and in the one mass scale dominance limit of $\Delta m^2_{21}/\Delta m^2_{31} \to 0$. There is some overlap of our work with Ref. [57], in which, also, unitarity violation was constrained using the $\nu_\mu \to \nu_\tau$ channel. However, we consider the possibility of combining several baselines, reducing the degeneracy of parameter space. To distinguish the nonunitarity signature with that from nonstandard interactions, the combination of the baselines is useful. When two or more observations suggest the same parameter region for scenarios with a nonunitary lepton mixing matrix, there can be stronger implications to determine the origin of the signal beyond the standard oscillation scenario.

The plan of the paper is as follows. In the next section we discuss the parametrization that we use for nonunitary mixing matrices and present the current constraints on unitarity violation. In Sec. III, assuming the mixing matrix to be nonunitary, we give simplified expressions for the oscillation probabilities in vacuum and matter. In Sec. IV we discuss the degeneracies in the oscillation probabilities. In Sec. V we give our numerical results on the allowed regions of the parameter space in the model with the nonunitary PMNS matrix. We conclude in Sec. VI.

II. NONUNITARY MIXING MATRICES AND CURRENT CONSTRAINTS

Since nonunitarity of mixing matrices is a generic feature of theories with heavy states which mix with the light neutrinos, we consider a picture that the mixing with one heavy state dominates the nonunitary effect to obtain simple analytic expressions for probability. In this case the full 4×4 mixing matrix is unitary but the 3×3 submatrix for light neutrinos is nonunitary. A 4×4 unitary matrix can be parametrized by 6 angles $\theta_{12,13,14,23,24,34}$ and three phases $\delta_{13,24,34}$. If the neutrinos are Majorana in nature, then three additional phases can be present. We parametrize the 4×4 unitary matrix in the usual way in terms of the rotation matrices R_{ij}

$$\mathcal{U} = \tilde{R}_{34}\tilde{R}_{24}R_{14}R_{23}\tilde{R}_{13}R_{12}P, \tag{1}$$

where the R_{ij} represent rotations in ij generation space, for instance:

$$\tilde{R}_{34} = \begin{pmatrix} 1 & 0 & 0 & 0 \\ 0 & 1 & 0 & 0 \\ 0 & 0 & c_{34} & s_{34}e^{-i\delta_{34}} \\ 0 & 0 & -s_{34}e^{i\delta_{34}} & c_{34} \end{pmatrix} \quad \text{or}$$
$$R_{14} = \begin{pmatrix} c_{14} & 0 & 0 & s_{14} \\ 0 & 1 & 0 & 0 \\ 0 & 0 & 1 & 0 \\ -s_{14} & 0 & 0 & c_{14} \end{pmatrix}, \tag{2}$$

with the usual notation $s_{ij} = \sin\theta_{ij}$ and $c_{ij} = \cos\theta_{ij}$. The symbol tilde means the mixing matrix including the CP phase. The diagonal matrix P contains the three Majorana phases, which we denote as α, β and γ:

$$P = \mathrm{diag}(1, e^{-i\alpha/2}, e^{-i(\beta/2-\delta_{13})}, e^{-i(\gamma/2-\delta_{34})}). \tag{3}$$

Since the Majorana phases are not important for oscillation studies, henceforth we will omit the matrix P.

Assuming the mixing of the fourth heavy state to be small, the above equation can be expanded in terms of small parameters ϵ_e, ϵ_μ and ϵ_τ characterizing the 14, 24 and 34 rotations, respectively.[2] With this simplification Eq. (1) can be expressed as

[2]We use $\cos\theta_{ij} = \cos\theta_{ji} \simeq 1 - \epsilon^2_\alpha/2$ and $\sin\theta_{ij} = -\sin\theta_{ji} \simeq \epsilon_\alpha$, where α is the corresponding index, e, μ or τ.

$$\mathcal{U} = \begin{pmatrix} & & \epsilon_e \\ & W & e^{-i\delta_{24}}\epsilon_\mu \\ & & e^{-i\delta_{34}}\epsilon_\tau \\ \mathcal{U}_{s1} & \mathcal{U}_{s2} & \mathcal{U}_{s3} \quad 1-\frac{1}{2}(\epsilon_e^2+\epsilon_\mu^2+\epsilon_\tau^2) \end{pmatrix}, \quad (4)$$

where W is the 3×3 nonunitary mixing matrix. This can be written as

$$W = \begin{pmatrix} U_{e1}(1-\epsilon_e^2/2) & U_{e2}(1-\epsilon_e^2/2) & U_{e3}(1-\epsilon_e^2/2) \\ U_{\mu 1}(1-\epsilon_\mu^2/2) & U_{\mu 2}(1-\epsilon_\mu^2/2) & U_{\mu 3}(1-\epsilon_\mu^2/2) \\ -e^{-i\delta_{24}}\epsilon_\mu\epsilon_e U_{e1} & -e^{-i\delta_{24}}\epsilon_\mu\epsilon_e U_{e2} & -e^{-i\delta_{24}}\epsilon_\mu\epsilon_e U_{e3} \\ U_{\tau 1}(1-\epsilon_\tau^2/2) & U_{\tau 2}(1-\epsilon_\tau^2/2) & U_{\tau 3}(1-\epsilon_\tau^2/2) \\ -e^{-i\delta_{34}}\epsilon_e\epsilon_\tau U_{e1} & -e^{-i\delta_{34}}\epsilon_e\epsilon_\tau U_{e2} & -e^{-i\delta_{34}}\epsilon_e\epsilon_\tau U_{e3} \\ -e^{i\phi}\epsilon_\mu\epsilon_\tau U_{\mu 1} & -e^{i\phi}\epsilon_\mu\epsilon_\tau U_{\mu 2} & -e^{i\phi}\epsilon_\mu\epsilon_\tau U_{\mu 3} \end{pmatrix}, \quad (5)$$

where $\phi = \delta_{24} - \delta_{34}$, $\mathcal{U}_{sk} = -\epsilon_e U_{ek} - e^{i\delta_{24}}\epsilon_\mu U_{\mu k} - e^{i\delta_{34}}\epsilon_\tau U_{\tau k}$, and the 3×3 matrix $U_{\alpha i}$ with $\alpha = e, \mu, \tau$ and $i = 1, 2, 3$ is defined and parameterized as the usual unitary PMNS matrix for three generations.

Bounds on the moduli of the unitarity violation parameters can come from electroweak processes and from neutrino oscillations. The bounds obtained from present neutrino oscillation experiments are weaker than those obtained from electroweak decays [22]. Constraint on $\sum_{i=1}^3 W_{\alpha i}W_{\beta i}^*$ comes from rare decays of charged leptons $l_\alpha \to l_\beta\gamma$ [21,22,38,39,42,43], whereas $\sum_{i=1}^3 |W_{\alpha i}|^2$ can be constrained from processes like $W \to l\nu$, $Z \to \nu\bar{\nu}$. Constraints on the diagonal elements of the nonunitary matrix can also come from tests for lepton universality [21,22,42,43]. At present there is strict constraint on light-heavy mixing in the $e-\mu$ sector coming from nonobservation of the decay $\mu \to e\gamma$. For nonunitarity induced through heavy right-handed neutrinos the bound quoted in Refs. [38,39] is

$$\left|\sum_{i=1}^3 W_{ei}W_{\mu i}^*\right| \equiv \epsilon_e\epsilon_\mu \lesssim 1.2\times 10^{-4}. \quad (6)$$

The bound on the $\mu-\tau$ sector is much weaker:

$$\left|\sum_{i=1}^3 W_{\mu i}W_{\tau i}^*\right| \equiv \epsilon_\mu\epsilon_\tau \lesssim 2\times 10^{-2}. \quad (7)$$

The ϵ_α's are also constrained by electroweak measurements individually as [36,51]

$$\epsilon_e^2 < 0.012, \qquad \epsilon_\mu^2 < 0.0096, \qquad \epsilon_\tau^2 < 0.016. \quad (8)$$

Although we parametrize our nonunitary mixing matrix assuming one heavy state to dominate for the sake of simplicity, it is possible to generalize this discussion to more complicated mixing structures between the three light and more than one heavy states. In this case the entries appearing in the fourth row and column of the matrix $\mathcal{U}$ appearing in Eq. (4) will be replaced by matrices [61]. However, the main part of our discussion will not change. We will touch on this point at the beginning of Sec. III A, showing the general expression of the oscillation probability.

III. CALCULATION OF OSCILLATION PROBABILITIES

A. Oscillation probability in vacuum

The most general expression of survival/oscillation probability for $\nu_\alpha \to \nu_\beta$ in vacuum without assuming unitarity of mixing matrices is [53]

$$P_{\nu_\alpha\to\nu_\beta} = \frac{1}{N_\alpha N_\beta} \times \left\{ \left| \sum_{i=1}^{\text{light}} W_{\beta i}W_{\alpha i}^* \right|^2 - 4\sum_{i<j}^{\text{light}} R_{\alpha\beta}^{ij}\sin^2\frac{(m_j^2-m_i^2)L}{4E} - 2\sum_{i<j}^{\text{light}} I_{\alpha\beta}^{ij}\sin\frac{(m_j^2-m_i^2)L}{2E} \right\}, \quad (9)$$

where $N_\alpha = \sum_{i=1}^{\text{light}} |W_{\alpha i}|^2$, $R_{\alpha\beta}^{ij} = \text{Re}[W_{\beta i}W_{\alpha i}^*W_{\beta j}^*W_{\alpha j}]$, $I_{\alpha\beta}^{ij} = \text{Im}[W_{\beta i}W_{\alpha i}^*W_{\beta j}^*W_{\alpha j}]$, and the sum of the mass eigenstate index is taken over the states concerned with the neutrino propagation (which is mentioned as "light" here). Although we consider a 4×4 mixing matrix (for the three light mass eigenstates and one heavy one) in the previous section and in the rest of the paper, the above expression for probability can be applied to the more general case where W is the part of the larger unitary matrix rather than 4×4.

If we concentrate on baselines and energies such that the one mass scale dominance approximation can be employed, then the terms containing $\Delta m_{21}^2 L/(4E)$ can be neglected and the expression simplifies to

$$P_{\nu_\alpha\to\nu_\beta} = \frac{1}{N_\alpha N_\beta}\left\{ \left| \sum_{i=1}^{3} W_{\beta i}W_{\alpha i}^* \right|^2 - 4[R_{\alpha\beta}^{13} + R_{\alpha\beta}^{23}]\sin^2\frac{\Delta m_{31}^2 L}{4E} - 2[I_{\alpha\beta}^{13} + I_{\alpha\beta}^{23}] \times \sin\frac{\Delta m_{31}^2 L}{2E} \right\}. \quad (10)$$

In the standard oscillation framework, the last term does not exist. This has a different energy and baseline dependence from the standard oscillation term shown as the second term. This can be a characteristic signature of new physics in oscillation.

Now we simplify our discussion to the model with one heavy state. As mentioned in the previous section, there is already strong constraint on the combination of the parameters $\epsilon_e\epsilon_\mu$. Therefore we assume $\epsilon_e = 0$ throughout this article. With this assumption, the deviation of unitarity can occur in the $\nu_\mu \to \nu_\mu$, $\nu_\mu \to \nu_\tau$ and $\nu_\tau \to \nu_\tau$ channel.[3] In the limit of $\theta_{13} \to 0$ and $\Delta m^2_{21}/\Delta m^2_{31} \to 0$, the survival probability $P_{\nu_\mu\to\nu_\mu}$ can be expressed as

$$P_{\nu_\mu\to\nu_\mu} = 1 - \sin^2 2\theta_{23}\sin^2\frac{\Delta m^2_{31}L}{4E} + \mathcal{O}(\epsilon^3). \tag{11}$$

From this equation, we see that the second order of the nonunitary effects in each term cancels out with the normalization factor $1/N^2_\mu$. In the $\nu_\tau \to \nu_\tau$ channel also the nonunitary effect comes as a small correction to the standard oscillation term and the standard oscillation term dominates. On the other hand, the oscillation probability for $\nu_\mu \to \nu_\tau$ is approximated as

$$\begin{aligned} P_{\nu_\mu\to\nu_\tau} &= \{\epsilon^2_\mu\epsilon^2_\tau + \mathcal{O}(\epsilon^5)\} + \sin 2\theta_{23}\{\sin 2\theta_{23} \\ &\quad + 2\epsilon_\mu\epsilon_\tau\cos 2\theta_{23}\cos\phi + \mathcal{O}(\epsilon^3)\}\sin^2\frac{\Delta m^2_{31}L}{4E} \\ &\quad + \{\epsilon_\mu\epsilon_\tau\sin\phi\,\sin 2\theta_{23} + \mathcal{O}(\epsilon^3)\}\sin\frac{\Delta m^2_{31}L}{2E} \\ &\quad + \mathcal{O}(s_{13}) + \mathcal{O}(\Delta m^2_{21}/\Delta m^2_{31}). \end{aligned} \tag{12}$$

The term with $\sin\phi$ takes a different energy dependence from the standard oscillation term. Therefore, we can expect that this can be distinguished from the standard oscillation signals. The term of $\mathcal{O}(\epsilon^2)$ in the standard oscillation term [$\sin^2\Delta m^2_{31}L/(4E)$ term] cannot be important because it is always smaller enough than the standard contribution $\sin^2 2\theta_{23}$. Assuming $L = 130$ km, $E = 50$ GeV, and $\epsilon_\mu\epsilon_\tau = 10^{-2}$, the order of each term is calculated to be

$$\text{standard oscillation term}: \sin^2\frac{\Delta m^2_{31}L}{4E} \sim 6.8\times 10^{-5}, \tag{13}$$

$$\sin\phi \text{ term}: \epsilon_\mu\epsilon_\tau\sin\frac{\Delta m^2_{31}L}{2E} \sim 1.7\times 10^{-4}, \tag{14}$$

$$\text{zero-distance term}: \epsilon^2_\mu\epsilon^2_\tau = 10^{-4}, \tag{15}$$

and the three terms in Eq. (12) are thus of the same order of magnitude and this channel provides a better option for probing violation of unitarity.

The noteworthy feature of the above equation is the zero-distance term $\epsilon^2_\mu\epsilon^2_\tau$. Consequently for a near detector one gets,

$$P^{\text{near}}_{\nu_\mu\to\nu_\tau} = \epsilon^2_\mu\epsilon^2_\tau. \tag{16}$$

It is actually very small. However, there are two positive aspects: (i) a huge number of neutrinos comes into the near detector and (ii) the background for this process, i.e., the standard oscillation events, is highly suppressed.

We have not shown the θ_{13} and Δm^2_{21} dependent terms explicitly in the analytic expressions. These can be found in Ref. [62]. We note that the presence of these terms does not change our discussion. The terms characterizing the nonunitary effect take a quite different energy dependence from the terms containing θ_{13} and Δm^2_{21}. The latter terms are more suppressed in the high energy limit with which we deal in this study. Nevertheless in the numerical calculations we have included nonzero values of θ_{13} and Δm^2_{21}.

B. Oscillation probability in matter

When we introduce the nonunitary PMNS matrix, neutrinos obtain additional matter effect mediated by neutral current interactions [54–56].[4] For nonunitary mixing, the $\nu_\mu \to \nu_\tau$ oscillation probability in matter of constant density in the simplifying approximation of $\theta_{13} \to 0$ and $\Delta m^2_{21}/\Delta m^2_{31} \to 0$ can be expressed as

$$\begin{aligned} P_{\nu_\mu\to\nu_\tau} &= \sin 2\theta_{23}(\sin 2\theta_{23} + 2\epsilon_\mu\epsilon_\tau\cos 2\theta_{23}\cos\phi)\sin^2\frac{\Delta m^2_{31}L}{4E} + \epsilon_\mu\epsilon_\tau\sin\phi\,\sin 2\theta_{23}\sin\frac{\Delta m^2_{31}L}{2E} \\ &\quad - \epsilon_\mu\epsilon_\tau\left(\frac{a_{\text{NC}}L}{2E}\right)\sin^3 2\theta_{23}\cos\phi\,\sin\frac{\Delta m^2_{31}L}{2E} - 4\epsilon_\mu\epsilon_\tau\left(\frac{a_{\text{NC}}}{\Delta m^2_{31}}\right)\sin 2\theta_{23}\cos^2 2\theta_{23}\cos\phi\sin^2\frac{\Delta m^2_{31}L}{4E} \\ &\quad - 2\left(\frac{a_{\text{NC}}}{\Delta m^2_{31}}\right)\sin^2 2\theta_{23}\cos 2\theta_{23}(\epsilon^2_\mu - \epsilon^2_\tau)\sin^2\frac{\Delta m^2_{31}L}{4E} + \left(\frac{a_{\text{NC}}L}{4E}\right)\sin^2\theta_{23}\cos 2\theta_{23}(\epsilon^2_\mu - \epsilon^2_\tau)\sin\frac{\Delta m^2_{31}L}{2E} \\ &\quad + \mathcal{O}(\epsilon^3) + \mathcal{O}(s_{13}) + \mathcal{O}(\Delta m^2_{21}/\Delta m^2_{31}), \end{aligned} \tag{17}$$

where a_{NC} is the matter effect mediated by neutral current interaction. This is consistent with the result shown in Ref. [56]

[3]Alternatively one can study the violation of unitarity in both the $\nu_e \to \nu_\tau$ channel and $\nu_\mu \to \nu_\tau$ channel [57].
[4]The nonstandard matter effect mediated by neutral current interactions was also discussed in Ref. [63].

though the procedures used are somewhat different. Since $\theta_{23} \simeq \pi/4$, we can omit the terms which are proportional to $\cos 2\theta_{23}$, and finally, it is reduced to

$$P_{\nu_\mu \to \nu_\tau} = \sin^2 2\theta_{23} \sin^2 \frac{\Delta m^2_{31} L}{4E} + \epsilon_\mu \epsilon_\tau \sin 2\theta_{23} \sin\phi \sin \frac{\Delta m^2_{31} L}{2E} - \epsilon_\mu \epsilon_\tau \left(\frac{a_{\rm NC} L}{2E} \right) \sin^3 2\theta_{23} \cos\phi \sin \frac{\Delta m^2_{31} L}{2E}. \quad (18)$$

This formula can nicely explain the numerical result which will be shown in the following sections. We have an additional term in comparison with Eq. (12), which depends on $\cos\phi$ differing from the vacuum term. This is the key feature to resolve the degeneracies which will be explained in the next section. The details of the derivation are described in Appendix A.

IV. DEGENERACIES

From the expression Eq. (12) for the oscillation probability $P_{\nu_\mu \to \nu_\tau}$ in vacuum, we see that this is invariant under the following transformations:

(1) θ_{23} (octant) degeneracy: $P_{\nu_\mu \to \nu_\tau}(\theta_{23}) = P_{\nu_\mu \to \nu_\tau}(\pi/2 - \theta_{23})$,
(2) sign$[\Delta m^2_{31}]$-ϕ degeneracy: $P_{\nu_\mu \to \nu_\tau}(\Delta m^2_{31} > 0, \phi) = P_{\nu_\mu \to \nu_\tau}(\Delta m^2_{31} < 0, -\phi)$,
(3) ϕ-$(\pi - \phi)$ degeneracy: $P_{\nu_\mu \to \nu_\tau}(\phi) = P_{\nu_\mu \to \nu_\tau}(\pi - \phi)$,
(4) $(\epsilon_\mu \epsilon_\tau)$-$\phi$ degeneracy: $P_{\nu_\mu \to \nu_\tau}((\epsilon_\mu \epsilon_\tau), \phi) = P_{\nu_\mu \to \nu_\tau}((\epsilon_\mu \epsilon_\tau)', \phi')$.

Here, the values of oscillation parameters which are not explicitly shown are taken to be the same on both the sides of the equations. These can give rise to degeneracies in the $(\epsilon_\mu \epsilon_\tau)$-$\phi$ plane even in the limit $\theta_{13} \to 0$. Below we discuss these degeneracies. If θ_{13} is nonzero, then additional degeneracies due to δ_{CP} can also be there. But this will not give rise to any additional degenerate solutions in the $(\epsilon_\mu \epsilon_\tau)$-$\phi$ plane. The $(\epsilon_\mu \epsilon_\tau)$-$\phi$ degeneracy is similar to the θ_{13}-δ_{CP} intrinsic degeneracy and the sign$[\Delta m^2_{31}]$-ϕ degeneracy is same as the sign$[\Delta m^2_{31}]$-δ_{CP} degeneracy often discussed in the context of the golden channel measurements [64]. However, the ϕ-$(\pi - \phi)$ degeneracy comes due to the nonunitary effect and has no analog with degeneracies occurring due to the CP phase δ_{CP}. Note that in addition to the degeneracies $\epsilon_\mu \epsilon_\tau$ and ϕ occur in a correlated fashion in the oscillation probability shown in Eq. (12). The correlation is similar to that between θ_{13} and δ_{CP} in standard neutrino oscillation probabilities in the sense that they are the absolute values and their phases (for the CP-violating effect in oscillations, see, e.g., Ref. [64]). Hence the uncertainty in determination of one of these parameters can affect that of the other even for the same hierarchy. When we assume the maximal mixing for θ_{23}, the θ_{23} octant degeneracy is not present.

The expression Eq. (18) breaks some of the degeneracies. Because of the presence of the $\cos\phi$ term, induced by matter effect, sign$[\Delta m^2_{31}]$-ϕ and ϕ-$(\pi - \phi)$ degeneracies can be resolved if we can see this term. To do so, we have to go to the long baseline because the term is simply proportional to the baseline length. However, in the long baseline region, the standard oscillation term can be order one, and the tiny nonunitary effect could be easily absorbed by the standard oscillation term. The significance of the nonunitary matter effect should be checked numerically. The $(\epsilon_\mu \epsilon_\tau)$-$\phi$ correlation is present in the oscillation probability in matter as well.

We can illustrate the occurrence of degeneracies due to the invariances listed above by using the equiprobability plots [65]. Here, the standard oscillation parameters are fixed as

$$\sin^2\theta_{12} = 0.31, \quad \sin^2 2\theta_{13} = 10^{-2}, \quad \delta_{CP} = 0, \quad |\Delta m^2_{31}| = 2.5 \times 10^{-3}\ [\mathrm{eV}^2], \quad \Delta m^2_{21} = 7.9 \times 10^{-5}\ [\mathrm{eV}^2], \quad (19)$$

and θ_{23} and the sign of the atmospheric mass square difference will be given later. For the nonunitary parameters, we adopt

$$(\epsilon_\mu \epsilon_\tau)^{\rm true} = 10^{-2}, \quad \phi^{\rm true} = \pi/4 \quad (20)$$

as the reference values throughout this paper.[5] The above value of $(\epsilon_\mu \epsilon_\tau)$ is allowed from the current bound and within the reach of future collider experiments [37]. The large light-heavy mixing is preferred from the successful leptogenesis in the models with the right-handed neutrinos with TeV scale masses. The equiprobability curves shown in the following mean that the condition

$$P_{\nu_\mu \to \nu_\tau}((\epsilon_\mu \epsilon_\tau)^{\rm fit}, \phi^{\rm fit}) = P_{\nu_\mu \to \nu_\tau}((\epsilon_\mu \epsilon_\tau)^{\rm true}, \phi^{\rm true}) \quad (21)$$

is fulfilled on each curve.

The left panel in Fig. 1 is for the θ_{23} degeneracy. The plot is done for $E = 50$ GeV, and the baseline is taken to be 130 km with 2.7 g/cm^3 as the matter density although matter effect is not relevant in this setup. In this plot we draw equiprobability contours in the $(\epsilon_\mu \epsilon_\tau)$-$\phi$ plane for two values of θ_{23},

$$\sin^2\theta_{23} = \{0.64, 0.36\}. \quad (22)$$

Here we assume the NH mass spectrum. The plot shows that the curve with $\sin^2\theta_{23} = 0.64$ (thin solid) completely

[5] More precisely, we take $\epsilon_\mu^{\rm true} = \epsilon_\tau^{\rm true} = 0.1$ in our numerical calculations. This allocation does not affect the results since the leading contribution of the nonunitarity always appears as the combination $\epsilon_\mu \epsilon_\tau$.

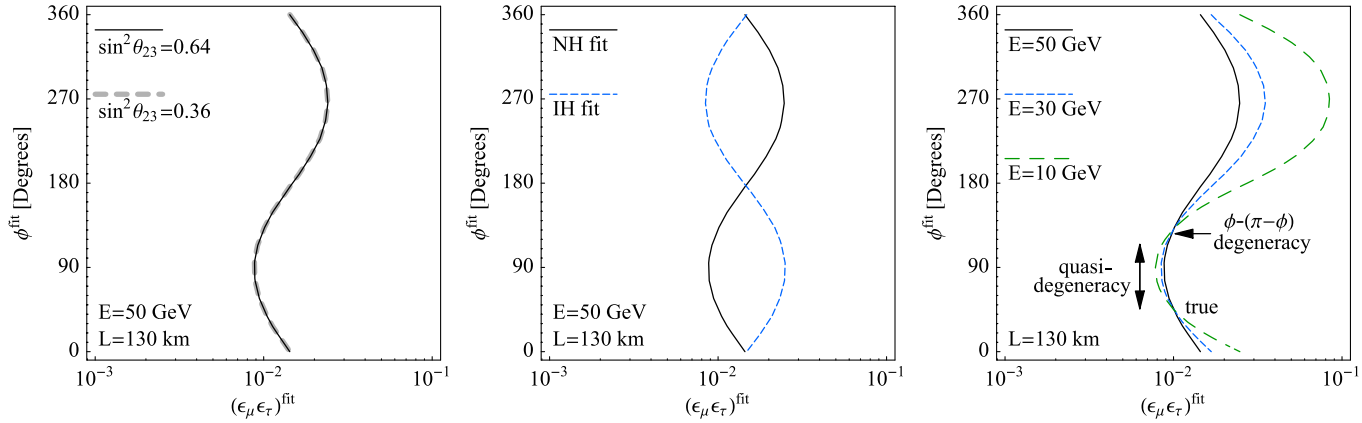

FIG. 1 (color online). Equiprobability plots for θ_{23} degeneracy (left), for the sign of Δm^2_{31} degeneracy (center), and for ϕ-$(\pi-\phi)$ degeneracy and $\epsilon_\mu\epsilon_\tau$-$\phi$ correlation (right). The neutrino energy is taken to be 50 GeV and the source-detector distance is 130 km.

coincides with that of $\sin^2\theta_{23} = 0.36$ (thick dashed gray), and these two cannot be distinguished. However, this degeneracy does not give rise to any additional regions in the $(\epsilon_\mu\epsilon_\tau)$-$\phi$ parameter plane because this degeneracy is not due to the nonunitary parameters; i.e., the degenerate solutions take the same values of $(\epsilon_\mu\epsilon_\tau)$ and ϕ on both sides of Eq. (21),

$$P_{\nu_\mu\to\nu_\tau}(\theta_{23}, (\epsilon_\mu\epsilon_\tau), \phi) = P_{\nu_\mu\to\nu_\tau}(\pi/2-\theta_{23}, (\epsilon_\mu\epsilon_\tau), \phi). \tag{23}$$

The middle panel in Fig. 1 is for the degeneracy on the sign $[\Delta m^2_{31}]$-ϕ. The solid curve is similar to the curves in the left panel. Here, the standard oscillation parameters are again taken to be the values in Eq. (19) but $\sin^2\theta_{23}$ is assumed to be 0.5, and the NH is adopted on both sides of Eq. (21). In the calculation of the dashed (blue) curve, the true probability with NH is fitted by the probability with the IH mass spectrum. Therefore, the condition which is satisfied on the dashed curve is written as

$$P_{\nu_\mu\to\nu_\tau}((\epsilon_\mu\epsilon_\tau)^{\rm fit}, \phi^{\rm fit}, {\rm IH}) = P_{\nu_\mu\to\nu_\tau}((\epsilon_\mu\epsilon_\tau)^{\rm true}, \phi^{\rm true}, {\rm NH}). \tag{24}$$

Although the dashed curve does not pass through the true value point which is shown as the black dot in the plot, the true oscillation probability can also be reproduced on it. The shape of the dashed curve is the reflection of the solid curve at the $\phi = 0$ point.

The right panel in Fig. 1 illustrates the ϕ-$(\pi-\phi)$ degeneracy and the $(\epsilon_\mu\epsilon_\tau)$-$\phi$ *quasi*degeneracy. On each curve, the condition

$$P_{\nu_\mu\to\nu_\tau}((\epsilon_\mu\epsilon_\tau)^{\rm fit}, \phi^{\rm fit}, E) = P_{\nu_\mu\to\nu_\tau}((\epsilon_\mu\epsilon_\tau)^{\rm true}, \phi^{\rm true}, E) \tag{25}$$

is satisfied, where the values of the standard oscillation parameters are again taken as shown in Eq. (19), and the maximal mixing for θ_{23} and the NH are assumed on both sides of Eq. (25). We plot the curves of three cases with the following neutrino energies:

$$E = \{10, 30, 50\} \qquad [{\rm GeV}]. \tag{26}$$

For a fixed energy all the points on the curve give the same probability reflecting the $(\epsilon_\mu\epsilon_\tau)$-$\phi$ degeneracy. However, if one considers other illustrative values of energies and draws the corresponding equiprobability curves passing through the true value point, then in a large region of parameter space, the equiprobability curves trace different paths. Consequently in these regions the $(\epsilon_\mu\epsilon_\tau)$-$\phi$ degeneracy can be removed by adding the spectral information. However, the figure also shows that the three curves cross at two points: one is the true value point (shown as the black dot), and the other is the fake solution which is referred to above as the ϕ-$(\pi-\phi)$ degeneracy for each curve. We can also find that at the region between the true solution and the fake solution, all three curves take a quite similar path indicating that in this region the different probabilities for different energies have very little dependence on parameters. This means that it is hard to resolve the solutions at this region even with spectral information and hence we mention this as the *quasi*degeneracy. We can draw a plot similar to Fig. 1 with IH as the true hierarchy.

In Fig. 2 we plot the equiprobability plot for a neutrino of energy 50 GeV and $L = 3000$ km. The true hierarchy is assumed to be NH and the true value point is again shown as a black dot in the figure. The dashed line shows the plot for the IH fit, on which the true oscillation probability can be reproduced. There are two points at which the NH and IH probabilities cross each other. The conditions for obtaining these points can be worked out from the expression Eq. (18). In general the condition for degeneracy on these curves can be written as

$$P_{\nu_\mu\to\nu_\tau}((\epsilon_\mu\epsilon_\tau), \phi, {\rm NH}) = P_{\nu_\mu\to\nu_\tau}((\epsilon_\mu\epsilon_\tau)', \phi', {\rm IH}). \tag{27}$$

At the point where the NH and IH curves cross, the $\epsilon_\mu\epsilon_\tau$ and ϕ are the same for both NH and IH. This gives

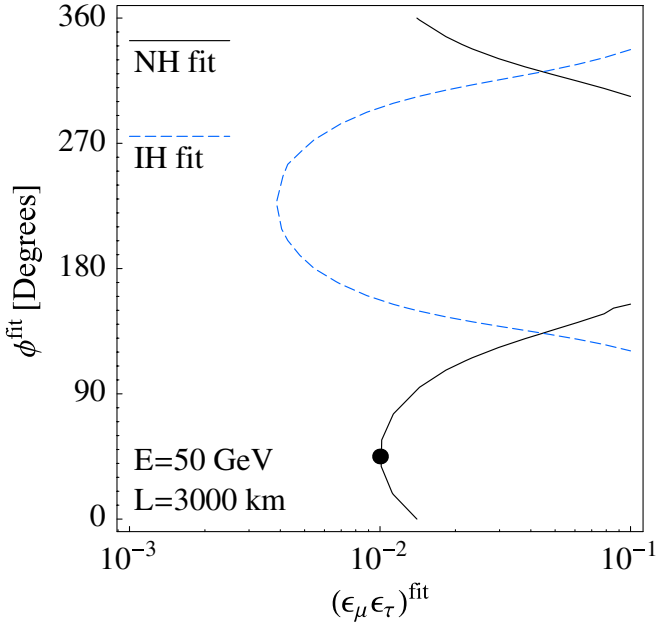

FIG. 2 (color online). Equiprobability plot for $E = 50$ GeV and $L = 3000$ km. The solid line denotes the NH fit and the dashed line denotes the IH fit. The true value of $(\epsilon_\mu\epsilon_\tau)$ and ϕ is marked by the black dot. The standard oscillation parameters are taken to be the values shown in Eq. (19) and θ_{23} is assumed to be maximal.

$$\tan\phi = \frac{a_{\rm NC}L}{2E}. \tag{28}$$

For $L = 3000$ km and $E = 50$ GeV, the above gives $\phi \approx 140^\circ$ and $\pi + 140^\circ$ as obtained in the figure.

V. NUMERICAL RESULTS: ALLOWED REGION ON THE $(\epsilon_\mu\epsilon_\tau)$-$\phi$ PLANE

In this section we present the results of our numerical analysis. We first present the allowed regions in the $(\epsilon_\mu\epsilon_\tau)$-$\phi$ plane for an OPERA-like detector at a distance of 130 km from a neutrino factory source and describe how the degeneracies are realized. This experimental setup has already been examined in Ref. [57]. However, we will pay attention to the degeneracy of the solutions. Later, we will see that how these degenerate solutions are resolved, including information on matter effect.

In Fig. 3, we plot the χ^2 function which is defined as[6]

$$\chi^2((\epsilon_\mu\epsilon_\tau)^{\rm fit}, \phi^{\rm fit}) = \min_{\lambda^{\rm fit}} \sum_i^{\rm bin} |N_i(\lambda^{\rm true}, (\epsilon_\mu\epsilon_\tau)^{\rm true}, \phi^{\rm true}) - N_i(\lambda^{\rm fit}, (\epsilon_\mu\epsilon_\tau)^{\rm fit}, \phi^{\rm fit})|^2/V_i, \tag{29}$$

where N_i is the neutrino event number in the ith energy bin, λ represents the standard oscillation parameters and V_i is the variance which is appropriately defined to include the statistical and systematic errors. Here we adopt the values shown in Eq. (19) for the standard oscillation parameters. Since it is not possible to resolve the θ_{23} degeneracy in this experiment (in the $\nu_\mu \to \nu_\tau$ channel), we take the reference true values for θ_{23} as the maximal. The true mass hierarchy is assumed to be NH. The parameters for the nonunitary nature are taken as shown in Eq. (20). The left panel in Fig. 3 shows the allowed region in the $(\epsilon_\mu\epsilon_\tau)$-$\phi$ plane. As discussed earlier, since the probability in this case is a function of $\sin^2 2\theta_{23}$, the θ_{23} octant degeneracy does not give rise to any additional regions in the $(\epsilon_\mu\epsilon_\tau)$-$\phi$ plane and the solutions for true θ_{23} and wrong θ_{23} occur in the same place. Here the two solutions (two crescent regions) correspond to two choices for the sign of Δm^2_{31} in the fit event. The figure also shows that for each hierarchy there is the ϕ-$(\pi - \phi)$ degeneracy. The spurious solution corresponding to $(\epsilon_\mu\epsilon_\tau)$-$\phi$ degeneracy is removed by using the spectrum information. There is a weak negative correlation between $\epsilon_\mu\epsilon_\tau$ and ϕ for each allowed zone. We next discuss how one can eliminate the degenerate solutions in the $(\epsilon_\mu\epsilon_\tau)$-$\phi$ plane by combining the experiments at various baselines. The remaining degeneracies are the sign$[\Delta m^2_{31}]$-ϕ degeneracy, the ϕ-$(\pi - \phi)$ degeneracy and the $(\epsilon_\mu\epsilon_\tau)$-$\phi$ quasidegeneracy. The right plot of Fig. 3 shows the combined results of an OPERA-like detector at 130 km baseline and a 0.1 kt liquid argon (LAr) type near detector which is located at $L = 2$ km.[7] The probability at the near detector depends on $\epsilon_\mu\epsilon_\tau$ only. Thus combining with this experiment helps to narrow down the allowed region but the degeneracies still exist. The correlation between ϕ and $\epsilon_\mu\epsilon_\tau$ is now almost vanishing.

In the left panel of Fig. 4 we plot the allowed regions for the combination of a neutrino factory and a 100 kt LAr type far detector which is located at $L = 3000$ km. A comparison of this figure with the equiprobability plot in Fig. 2 reveals that the middle region of both the panels in Fig. 4 corresponds to the IH fit. As discussed in the previous section the main contribution of matter effect depends on $\cos\phi$ which is different from the case in vacuum. Therefore, the ϕ-$(\pi - \phi)$ degeneracy as well as sign$[\Delta m^2_{31}]$-ϕ degeneracy can be removed by this matter term. This is reflected in the figure. However, the probabilities for NH and IH can still be equal when the condition Eq. (27) is satisfied. This gives rise to the middle region in Fig. 4. There is a positive correlation in this case between $\epsilon_\mu\epsilon_\tau$ and ϕ for each allowed region. The result combining the near detector is shown as the right panel in Fig. 4. This helps to reduce the uncertainty in the $\epsilon_\mu\epsilon_\tau$, and since ϕ is a

[6] In the actual implementation, we adopt the Poisson distribution, add the appropriately defined priors and marginalize also over the systematic parameters, following GLOBES software [66,67].

[7] A 0.1 kt LAr detector as a near detector has been discussed in Ref. [68].

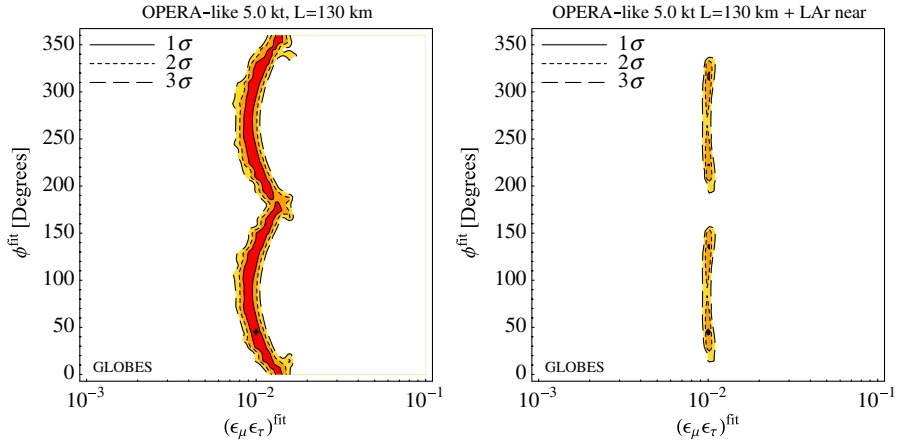

FIG. 3 (color online). Allowed regions in the $(\epsilon_\mu\epsilon_\tau)$-$\phi$ plane for an OPERA-like detector at a distance of 130 km from a neutrino factory source (left), and for the same setup but with a 0.1 kt liquid argon near detector (right).

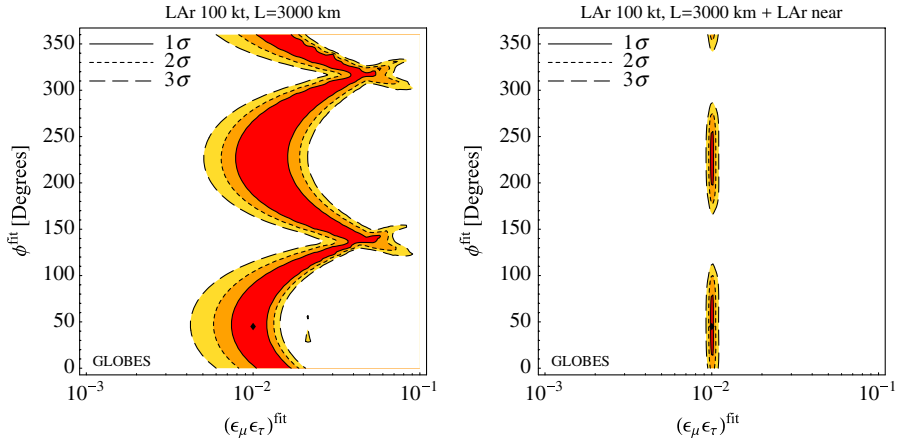

FIG. 4 (color online). Same as Fig. 3 but we assume a 100 kt LAr detector at $L = 3000$ km in the left panel. In the right panel, the same near detector as Fig. 3 is added.

variable correlated with $\epsilon_\mu\epsilon_\tau$, the uncertainty on ϕ is also reduced. Therefore, the allowed regions for each hierarchy become much narrower as compared to the left panel. The allowed regions now are almost parallel to the ϕ axis. The inclusion of the 3000 km removes the ϕ-$(\pi - \phi)$ degeneracy of Fig. 3 for each hierarchy. In addition, in such a long baseline experiment, it would be possible to obtain information on the sign$[\Delta m^2_{31}]$ from the other channels like $\nu_e \to \nu_\mu$. Including it, we could remove the wrong hierarchy solution and solve the all degeneracies.

VI. CONCLUSIONS

The nonunitary mixing matrix is a generic feature for theories with mixing between neutrinos and heavy states and provides a window to probe physics at a high scale. In this paper we have studied the possibility of probing the nonunitarity of the neutrino mixing matrix at neutrino factories. We considered the $\nu_\mu \to \nu_\tau$ channel and detectors at a distance of 2 km, 130 km and 3000 km from the source. We show that for the $\nu_\mu \to \nu_\tau$ channel at 130 km, there can be degenerate solutions even for $\theta_{13} = 0$ in the $(\epsilon_\mu\epsilon_\tau)$-$\phi$ plane where ϕ and $\epsilon_\mu\epsilon_\tau$ are the phase and moduli of the unitarity violation parameter. The degenerate solutions in the $(\epsilon_\mu\epsilon_\tau)$-$\phi$ plane are due to

(i) $(\Delta m^2_{31} > 0, \phi) \to (\Delta m^2_{31} < 0, -\phi)$
(ii) $\phi \to \pi - \phi$
(iii) $(\epsilon_\mu\epsilon_\tau, \phi) \to ((\epsilon_\mu\epsilon_\tau)', \phi')$

For a detector at a distance of 130 km from a neutrino factory source the last degeneracy can be removed using spectral information and no additional disconnected solution will appear. By adding an experiment at 2 km the correlation between ϕ and $\epsilon_\mu\epsilon_\tau$ can be reduced and the allowed ranges narrow down. For the 3000 km experiment the matter effects are relevant and this removes the first and second degeneracy listed above. However, although the hierarchy degeneracy listed above gets removed, there can still be the degeneracy where probabilities for NH and IH give same values. If we consider only the 3000 km experiment, then there is a greater correlation between

$\epsilon_\mu\epsilon_\tau$-$\phi$ and the allowed regions are larger as compared to the 130 km experiment. However, addition of the 2 km experiment to this reduces this correlation and the allowed regions become narrower. Although we have concentrated on the $\nu_\mu \to \nu_\tau$ channel in this study, if we combine the other channels like $\nu_e \to \nu_\mu$, we can obtain information on the hierarchy and then the allowed regions further reduce in size.

ACKNOWLEDGMENTS

We would like to thank A. Bandyopadhyay, P. Ghoshal, J. Kopp, W. Rodejohann, R. Singh and S. Umashankar for useful discussions and gratefully acknowledge M. Lindner and the particle and astroparticle physics group in the Max-Planck-Institut für Kernphysik for hospitality. S. G. acknowledges the Alexander-von-Humboldt Foundation and the XIth plan neutrino project of Harish-Chandra Research Institute for support.

APPENDIX A: ANALYTIC FORMULAS

In this section, we derive the expression of $\nu_\mu \to \nu_\tau$ oscillation probability in matter of constant density under some simplifying assumptions. If the neutrino mixing matrix is nonunitary, then although we can get the canonical form of the kinetic energy in the mass basis in terms of the flavor states, the kinetic term is not diagonal. Therefore it is more appropriate here to consider the neutrino propagation equation in the mass basis. The neutrino propagation Hamiltonian in matter can be generally represented in the vacuum mass eigenbasis as follows:

$$H_{ij} = \frac{1}{2E}\left\{\begin{pmatrix} 0 & & \\ & \Delta m^2_{21} & \\ & & \Delta m^2_{31}\end{pmatrix} + a_{\rm CC}\begin{pmatrix} |W_{e1}|^2 & W^*_{e1}W_{e2} & W^*_{e1}W_{e2} \\ W^*_{e2}W_{1e} & |W_{e2}|^2 & W^*_{e2}W_{e3} \\ W^*_{e3}W_{1e} & W^*_{e3}W_{e2} & |W_{e3}|^2\end{pmatrix} + a_{\rm NC}\begin{pmatrix} \sum_{\gamma=e,\mu,\tau}|W_{\gamma1}|^2 & \sum_{\gamma=e,\mu,\tau}W^*_{\gamma1}W_{\gamma2} & \sum_{\gamma=e,\mu,\tau}W^*_{\gamma1}W_{\gamma3} \\ \sum_{\gamma=e,\mu,\tau}W^*_{\gamma2}W_{\gamma1} & \sum_{\gamma=e,\mu,\tau}|W_{\gamma2}|^2 & \sum_{\gamma=e,\mu,\tau}W^*_{\gamma2}W_{\gamma3} \\ \sum_{\gamma=e,\mu,\tau}W^*_{\gamma3}W_{\gamma1} & \sum_{\gamma=e,\mu,\tau}W^*_{\gamma3}W_{2\gamma} & \sum_{\gamma=e,\mu,\tau}|W_{\gamma3}|^2\end{pmatrix}\right\}, \tag{A1}$$

where $a_{\rm CC} \equiv 2\sqrt{2}EG_Fn_e$, $a_{\rm NC} \equiv -\sqrt{2}EG_Fn_N = -a_{\rm CC}/2$ are the charged and neutral current potentials, respectively. We obtain simplified analytic expressions for the probability by solving the above equations in the limit $\theta_{13} \to 0$, $\Delta m^2_{21}/\Delta m^2_{31} \to 0$. In this limit the propagation Hamiltonian in the vacuum mass eigenbasis is

$$H_{ij} = (H_0)_{ij} + (H_{\epsilon_\mu\epsilon_\tau})_{ij} + (H_{\epsilon^2_\mu})_{ij} + (H_{\epsilon^2_\tau})_{ij}, \tag{A2}$$

where

$$(H_0)_{ij} = \frac{1}{2E}\left\{\begin{pmatrix} 0 & & \\ & 0 & \\ & & \Delta m^2_{31}\end{pmatrix} + a_{\rm CC}\begin{pmatrix} c^2_{12} & c_{12}s_{12} & 0 \\ c_{12}s_{12} & s^2_{12} & 0 \\ 0 & 0 & 0\end{pmatrix}\right\}, \tag{A3}$$

$$(H_{\epsilon_\mu\epsilon_\tau})_{ij} = -\frac{a_{\rm NC}}{2E}\epsilon_\mu\epsilon_\tau\begin{pmatrix} 2c_{23}s_{23}s^2_{12}c_\phi & -2c_{23}s_{23}c_{12}s_{12}c_\phi & s_{12}(c^2_{23}e^{-i\phi} - s^2_{23}e^{i\phi}) \\ -2c_{23}s_{23}c_{12}s_{12}c_\phi & 2c_{23}s_{23}c^2_{12}c_\phi & -c_{12}(c^2_{23}e^{-i\phi} - s^2_{23}e^{i\phi}) \\ s_{12}(c^2_{23}e^{i\phi} - s^2_{23}e^{-i\phi}) & -c_{12}(c^2_{23}e^{i\phi} - s^2_{23}e^{-i\phi}) & -2c_{23}s_{23}c_\phi\end{pmatrix}, \tag{A4}$$

$$(H_{\epsilon^2_\mu})_{ij} = -\frac{a_{\rm NC}}{2E}\epsilon^2_\mu\begin{pmatrix} s^2_{12}c^2_{23} & -s_{12}c_{12}c^2_{23} & -s_{12}s_{23}c_{23} \\ -s_{12}c_{12}c^2_{23} & c^2_{12}c^2_{23} & c_{12}s_{23}c_{23} \\ -s_{12}s_{23}c_{23} & c_{12}s_{23}c_{23} & s^2_{23}\end{pmatrix}, \tag{A5}$$

$$(H_{\epsilon^2_\tau})_{ij} = -\frac{a_{\rm NC}}{2E}\epsilon^2_\tau\begin{pmatrix} s^2_{12}s^2_{23} & -s_{12}c_{12}s^2_{23} & s_{12}s_{23}c_{23} \\ -s_{12}c_{12}s^2_{23} & c^2_{12}s^2_{23} & -c_{12}s_{23}c_{23} \\ s_{12}s_{23}c_{23} & -c_{12}s_{23}c_{23} & c^2_{23}\end{pmatrix}, \tag{A6}$$

up to the second order of the epsilon parameters. In writing the above a part proportional to the unit matrix is omitted as it contributes to the overall phase. The Hamiltonian is separated into two parts—(i) the zeroth order part H_0 which includes Δm^2_{31} and $a_{\rm CC}$ and (ii) perturbations $H_{\epsilon_\mu\epsilon_\tau}$, $H_{\epsilon^2_\mu}$ and $H_{\epsilon^2_\tau}$, induced by the nonunitarity. Note that the nonunitarity

effects appear always at the second order (or higher than that) of the ϵ_α parameters.

Treating $H_{\epsilon_\mu\epsilon_\tau}$, $H_{\epsilon_\mu^2}$ and $H_{\epsilon_\tau^2}$ as perturbations, the amplitude of the neutrino oscillation from a vacuum mass eigenstate ν_i to the other vacuum mass eigenstate ν_j can be written as

$$S_{ji} = (S_0)_{ji} + (S_{\epsilon_\mu\epsilon_\tau})_{ji} + (S_{\epsilon_\mu^2})_{ji}, +(S_{\epsilon_\tau^2})_{ji}, \tag{A7}$$

where S_0 is the zeroth order part, and $S_{\epsilon_\mu\epsilon_\tau}$, $S_{\epsilon_\mu^2}$ and $S_{\epsilon_\tau^2}$ correspond to the amplitudes with perturbations of $H_{\epsilon_\mu\epsilon_\tau}$, $H_{\epsilon_\mu^2}$ and $H_{\epsilon_\tau^2}$, respectively, which are calculated to be

$$(S_0)_{ji} = (\mathrm{e}^{-\mathrm{i}H_0L})_{ji}, \tag{A8}$$

$$(S_{\epsilon_\mu\epsilon_\tau})_{ji} = (\mathrm{e}^{-\mathrm{i}H_0L})_{jk}(-\mathrm{i})\int_0^L \mathrm{d}x(\mathrm{e}^{+\mathrm{i}H_0x})_{kl}(H_{\epsilon_\mu\epsilon_\tau})_{lm} \times (\mathrm{e}^{-\mathrm{i}H_0x})_{mi}, \tag{A9}$$

$$(S_{\epsilon_\mu^2})_{ji} = (\mathrm{e}^{-\mathrm{i}H_0L})_{jk}(-\mathrm{i})\int_0^L \mathrm{d}x(\mathrm{e}^{+\mathrm{i}H_0x})_{kl}(H_{\epsilon_\mu^2})_{lm} \times (\mathrm{e}^{-\mathrm{i}H_0x})_{mi}, \tag{10}$$

$$(S_{\epsilon_\tau^2})_{ji} = (\mathrm{e}^{-\mathrm{i}H_0L})_{jk}(-\mathrm{i})\int_0^L \mathrm{d}x(\mathrm{e}^{+\mathrm{i}H_0x})_{kl}(H_{\epsilon_\tau^2})_{lm}(\mathrm{e}^{-\mathrm{i}H_0x})_{mi}. \tag{A11}$$

Note that these amplitudes describe the transition between two vacuum mass eigenstates, ν_i and ν_j, and a transition between flavor states can be obtained by sandwiching these by the flavor states[8] which are described as [21,56,69]

$$|\nu_\alpha\rangle = \frac{1}{\sqrt{\sum_{j=1}^{\text{light}}|W_{\alpha j}|^2}}\sum_{i=1}^{\text{light}} W^*_{\alpha i}|\nu_i\rangle. \tag{A12}$$

The oscillation probability between the two flavor states ν_α and ν_β is derived as

$$\begin{aligned} P_{\nu_\alpha\to\nu_\beta} &= \left|\frac{1}{\sqrt{\sum_{l=1}^{\text{light}}|W_{\beta l}|^2}}W_{\beta j}(S_0 + S_{\epsilon_\mu\epsilon_\tau} + S_{\epsilon_\mu^2} + S_{\epsilon_\tau^2})_{ji} \right. \\ &\quad \left. \times \frac{1}{\sqrt{\sum_{k=1}^{\text{light}}|W_{\alpha k}|^2}}(W^\dagger)_{i\alpha}\right|^2 \\ &= \frac{1}{N_\alpha N_\beta}[|(S_0)_{\beta\alpha}|^2 + 2\mathrm{Re}[(S_0^*)_{\beta\alpha}(S_{\epsilon_\mu\epsilon_\tau})_{\beta\alpha}] \\ &\quad + 2\,\mathrm{Re}[(S_0^*)_{\beta\alpha}(S_{\epsilon_\mu^2})_{\beta\alpha}] \\ &\quad + 2\,\mathrm{Re}[(S_0^*)_{\beta\alpha}(S_{\epsilon_\tau^2})_{\beta\alpha}]] + \mathcal{O}(\epsilon^4), \end{aligned} \tag{A13}$$

[8]We underscore that, strictly speaking, this method has to be followed as it is not correct to write the neutrino propagation in the flavor basis because the flavor states do not form a complete set for the propagation Hamiltonian.

up to the first order perturbations. In the following, we will calculate each oscillation amplitude.

Diagonalizing the zeroth order Hamiltonian H_0, we obtain the mass squared eigenvalues and the mixing matrix $(V_0)_{i\tilde{j}}$ which connects the vacuum mass eigenbasis ν_i with the mass eigenbasis in matter $\nu_{\tilde{j}}$, and in the limit which we adopt here, they take the following simple forms

$$(H_0)_{\tilde{k}} = \mathrm{diag}(a_{\mathrm{CC}}, 0, \Delta m^2_{31}) = (V_0^\dagger)_{\tilde{k}j}(H_0)_{ji}(V_0)_{i\tilde{k}}, \tag{A14}$$

where

$$(V_0)_{i\tilde{j}} = \begin{pmatrix} c_{12} & -s_{12} & \\ s_{12} & c_{12} & \\ & & 1 \end{pmatrix}. \tag{A15}$$

Therefore, the zeroth order amplitude in the vacuum mass eigenbasis becomes

$$(S_0)_{ji} = (V_0)_{j\tilde{k}}\begin{pmatrix} \mathrm{e}^{-\mathrm{i}(a_{\mathrm{CC}}L/2E)} & & \\ & 1 & \\ & & \mathrm{e}^{-\mathrm{i}(\Delta m^2_{31}L/2E)} \end{pmatrix}(V_0^\dagger)_{\tilde{k}i}, \tag{A16}$$

and that for the transition between two flavor states is

$$(S_0)_{\beta\alpha} = W_{\beta j}(S_0)_{ji}(W^\dagger)_{i\alpha}. \tag{A17}$$

The oscillation probability at the zeroth order becomes

$$\begin{aligned} P^{0\text{th}}_{\nu_\mu\to\nu_\tau} &= \sin 2\theta_{23}(\sin 2\theta_{23} \\ &\quad + 2\epsilon_\mu\epsilon_\tau\cos 2\theta_{23}\cos\phi)\sin^2\frac{\Delta m^2_{31}L}{4E} \\ &\quad + \epsilon_\mu\epsilon_\tau\sin\phi\sin 2\theta_{23}\sin\frac{\Delta m^2_{31}L}{2E} + \mathcal{O}(\epsilon^3), \end{aligned} \tag{A18}$$

which is the same as the formula in the vacuum case.

Next, let us turn to the perturbation terms. The first one is the amplitude of $S_{\epsilon_\mu\epsilon_\tau}$. According to Eq. (A9), we can calculate it as

$$(S_{\epsilon_\mu\epsilon_\tau})_{ji} = \epsilon_\mu\epsilon_\tau\left(\mathrm{i}\frac{a_{\mathrm{NC}}}{2E}\right)(V_0)_{j\tilde{l}}\begin{pmatrix}0 & 0 & 0\\ 0 & -s_{2\times23}c_\phi L & \mathcal{A}\frac{2E}{i\Delta m^2_{31}}(1-\mathrm{e}^{-\mathrm{i}(\Delta m^2_{31}L/2E)})\\ 0 & \mathcal{A}^*\frac{2E}{i\Delta m^2_{31}}(1-\mathrm{e}^{-\mathrm{i}(\Delta m^2_{31}L/2E)}) & s_{2\times23}c_\phi L\mathrm{e}^{-\mathrm{i}(\Delta m^2_{31}L/2E)}\end{pmatrix}(V_0^\dagger)_{\tilde{k}i}, \tag{A19}$$

where the parameter $\mathcal{A}$ is defined as

$$\mathcal{A} \equiv (c^2_{23}\mathrm{e}^{-\mathrm{i}\phi} - s^2_{23}\mathrm{e}^{\mathrm{i}\phi}), \tag{A20}$$

and $s_{2\times23} \equiv \sin2\theta_{23}$. The amplitude for the $\nu_\mu \to \nu_\tau$ transition is reduced to

$$(S_{\epsilon_\mu\epsilon_\tau})_{\tau\mu} = \epsilon_\mu\epsilon_\tau\Big[\mathrm{i}\frac{a_{\mathrm{NC}}L}{4E}s^2_{2\times23}c_\phi(1+\mathrm{e}^{-\mathrm{i}(\Delta m^2_{31}L/2E)}) + \frac{a_{\mathrm{NC}}}{\Delta m^2_{31}}(\mathrm{e}^{\mathrm{i}\phi} - s^2_{2\times23}c_\phi)(1-\mathrm{e}^{-\mathrm{i}(\Delta m^2_{31}L/2E)})\Big] + \mathcal{O}(\epsilon^3). \tag{A21}$$

The contribution to the oscillation probability is calculated to be

$$2\,\mathrm{Re}[(S_0^*)_{\tau\mu}(S_{\epsilon_\mu\epsilon_\tau})_{\tau\mu}] = -\epsilon_\mu\epsilon_\tau\left(\frac{a_{\mathrm{NC}}L}{2E}\right)s^3_{2\times23}c_\phi\sin\frac{\Delta m^2_{31}L}{2E} - 4\epsilon_\mu\epsilon_\tau\left(\frac{a_{\mathrm{NC}}}{\Delta m^2_{31}}\right)s_{2\times23}c^2_{2\times23}c_\phi\sin^2\frac{\Delta m^2_{31}L}{4E}, \tag{A22}$$

up to the second order of the ϵ parameters. The contributions from $S_{\epsilon^2_\mu}$ and $S_{\epsilon^2_\tau}$ can also be calculated in the same way, which is

$$2\,\mathrm{Re}[(S_0^*)_{\tau\mu}(S_{\epsilon^2_\mu})_{\tau\mu}] + 2\,\mathrm{Re}[(S_0^*)_{\tau\mu}(S_{\epsilon^2_\tau})_{\tau\mu}] = \left(\frac{a_{\mathrm{NC}}L}{4E}\right)s^2_{2\times23}c_{2\times23}(\epsilon^2_\mu - \epsilon^2_\tau)\sin\frac{\Delta m^2_{31}L}{2E} - 2\left(\frac{a_{\mathrm{NC}}}{\Delta m^2_{31}}\right)s^2_{2\times23}c_{2\times23}(\epsilon^2_\mu - \epsilon^2_\tau)\sin^2\frac{\Delta m^2_{31}L}{4E}. \tag{A23}$$

From Eqs. (A18), (A22), and (A23), the oscillation probability for $\nu_\mu \to \nu_\tau$ in matter can be expressed as

$$\begin{aligned}P_{\nu_\mu\to\nu_\tau} = {}& \sin2\theta_{23}(\sin2\theta_{23} + 2\epsilon_\mu\epsilon_\tau\cos2\theta_{23}\cos\phi)\sin^2\frac{\Delta m^2_{31}L}{4E} + \epsilon_\mu\epsilon_\tau\sin\phi\sin2\theta_{23}\sin\frac{\Delta m^2_{31}L}{2E}\\ & - \epsilon_\mu\epsilon_\tau\left(\frac{a_{\mathrm{NC}}L}{2E}\right)\sin^3\!2\theta_{23}\cos\phi\sin\frac{\Delta m^2_{31}L}{2E} - 4\epsilon_\mu\epsilon_\tau\left(\frac{a_{\mathrm{NC}}}{\Delta m^2_{31}}\right)\sin2\theta_{23}\cos^2\!2\theta_{23}\cos\phi\sin^2\frac{\Delta m^2_{31}L}{4E}\\ & - 2\left(\frac{a_{\mathrm{NC}}}{\Delta m^2_{31}}\right)\sin^2\!2\theta_{23}\cos2\theta_{23}(\epsilon^2_\mu - \epsilon^2_\tau)\sin^2\frac{\Delta m^2_{31}L}{4E} + \left(\frac{a_{\mathrm{NC}}L}{4E}\right)\sin^2\theta_{23}\cos2\theta_{23}(\epsilon^2_\mu - \epsilon^2_\tau)\sin\frac{\Delta m^2_{31}L}{2E}\\ & + \mathcal{O}(\epsilon^3) + \mathcal{O}(s_{13}) + \mathcal{O}(\Delta m^2_{21}/\Delta m^2_{31}).\end{aligned} \tag{A24}$$

Since $\theta_{23} \simeq \pi/4$, we can omit the terms which are proportional to $\cos2\theta_{23}$, and finally, it reduces to

$$\begin{aligned}P_{\nu_\mu\to\nu_\tau} = {}& \sin^2\!2\theta_{23}\sin^2\frac{\Delta m^2_{31}L}{4E}\\ & + \epsilon_\mu\epsilon_\tau\sin2\theta_{23}\sin\phi\sin\frac{\Delta m^2_{31}L}{2E}\\ & - \epsilon_\mu\epsilon_\tau\left(\frac{a_{\mathrm{NC}}L}{2E}\right)\sin^3\!2\theta_{23}\cos\phi\sin\frac{\Delta m^2_{31}L}{2E}.\end{aligned} \tag{A25}$$

APPENDIX B: EXPERIMENTAL SETUPS IN NUMERICAL CALCULATIONS

The numerical work is performed using GLOBES software [66,67] which is modified for our purpose. We consider a neutrino factory as the source for ν_μ's based on NUFACT2 from Ref. [6]. The number of the decay muon is assumed to be 1.06×10^{21} per year and four years of running is being considered. Here, we concentrate on one polarity of the muon (μ^-). The stored muon is accelerated to 50 GeV.

We perform a binned χ^2 analysis with an energy window from 1 to 50 GeV and the width of each bin as 1 GeV. The signal event rate in the ith energy bin is calculated as

$$N_i^{\mathrm{signal}} = \int_{E_i-\Delta E/2}^{E_i+\Delta E/2}\mathrm{d}E'\int\mathrm{d}E_\nu\frac{\mathrm{d}\Phi(E_\nu)}{\mathrm{d}E_\nu}P_{\nu_\mu\to\nu_\tau}(E_\nu)\sigma_{\mathrm{CC}}(E_\nu) \times R(E_\nu, E')\epsilon_{\mathrm{eff}}, \tag{B1}$$

where $\mathrm{d}\Phi/\mathrm{d}E_\nu$ is the beam flux, σ_{CC} is the charged current cross section, ϵ_{eff} is the detection efficiency and R is the energy smearing function which is assumed to be the Gaussian distribution,

TABLE I. Rules for the experimental setup NuFACT + OPERA-like detector.

$\nu_\mu \to \nu_\tau$ Appearance			$\sigma_{\rm norm}$	$\sigma_{\rm cal}$
Signal	$0.1056 \otimes (\nu_\mu \to \nu_\tau)_{\rm CC}$		0.05	10^{-4}
Background	$3.414 \times 10^{-5} \otimes (\nu_\mu \to \nu_x)_{\rm NC}$	$3.414 \times 10^{-5} \otimes (\bar{\nu}_e \to \bar{\nu}_x)_{\rm NC}$	0.05	10^{-4}

TABLE II. Rules for the experimental setup NuFACT + LAr detector.

$\nu_\mu \to \nu_\tau$ Appearance			$\sigma_{\rm norm}$	$\sigma_{\rm cal}$
Signal	$0.0758 \otimes (\nu_\mu \to \nu_\tau)_{\rm CC}$		0.05	10^{-4}
Background	$8.502 \times 10^{-5} \otimes (\nu_\mu \to \nu_x)_{\rm NC}$	$8.502 \times 10^{-5} \otimes (\bar{\nu}_e \to \bar{\nu}_x)_{\rm NC}$	0.05	10^{-4}

$$R(E_\nu, E') = \frac{1}{\sigma(E_\nu)\sqrt{2\pi}} e^{-((E_\nu - E')^2/2\sigma^2(E_\nu))}, \qquad \text{(B2)}$$

with $\sigma \equiv 0.15 E_\nu$. E_ν is the neutrino beam energy and E' is the reconstructed energy. The errors for the event normalization $\sigma_{\rm norm}$ and so called tilt-error $\sigma_{\rm cal}$ are given in the following subsections. We consider three experimental setups.

1. NuFACT beam + OPERA-like detector with $L = 130$ km

We consider an OPERA-like detector at a distance of $L = 130$ km from a neutrino factory beam, which was examined in Ref. [57]. The detector mass is assumed to be 5.0 kt. The matter profile is assumed to be constant with the density 2.7 g/cm^3 although the matter effect itself is not significant in this setup.

For the signal detection efficiency, the errors and the backgrounds, we follow the glb file OPERA.glb. Since this glb file is designed for the CERN Neutrinos to Gran Sasso beam source, the numbers should be modified for the neutrino factory beam source. Here, we use the numbers shown in Table I.

2. NuFACT beam + LAr near detector

In this setup we consider a 0.1 kt liquid argon detector at 2 km away from the beam source, which has been discussed in Ref. [68]. Here we follow the glb file ICARUS.glb but modify the background estimation (see Table II).

3. NuFACT beam + large LAr far detector

In order to solve the ϕ-$(\pi - \phi)$ degeneracy and the $(\epsilon_\mu \epsilon_\tau)$-$\phi$ *quasi*degeneracy, it is effective to observe the matter effect coming from the nonunitary effect. To get the matter effect, we need a long baseline. Here, we set $L = 3000$ km and adopt 3.3 g/cm^3 as the matter density. However, in such a long baseline setup, we need a huge detector to collect enough event rates. We assume a 100 kt LAr detector whose rules are taken from ICARUS.glb, which is modified in the same manner as the LAr near detector setup.

[1] T. Schwetz, Phys. Scr. **T127**, 1 (2006).
[2] J. Bernabeu, S. Palomares-Ruiz, and S. T. Petcov, Nucl. Phys. **B669**, 255 (2003).
[3] R. Gandhi, P. Ghoshal, S. Goswami, P. Mehta, S. U. Sankar, and S. Shalgar, Phys. Rev. D **76**, 073012 (2007).
[4] R. Gandhi, P. Ghoshal, S. Goswami, P. Mehta, and S. Uma Sankar, Phys. Rev. D **73**, 053001 (2006).
[5] E. K. Akhmedov, M. Maltoni, and A. Y. Smirnov, J. High Energy Phys. 05 (2007) 077.
[6] P. Huber, M. Lindner, and W. Winter, Nucl. Phys. **B645**, 3 (2002).
[7] O. Mena, H. Nunokawa, and S. J. Parke, Phys. Rev. D **75**, 033002 (2007).
[8] R. Gandhi, P. Ghoshal, S. Goswami, P. Mehta, and S. Uma Sankar, arXiv:hep-ph/0506145.
[9] A. Samanta, arXiv:hep-ph/0610196.
[10] S. T. Petcov and T. Schwetz, Nucl. Phys. **B740**, 1 (2006).
[11] D. Indumathi and M. V. N. Murthy, Phys. Rev. D **71**, 013001 (2005).
[12] S. Palomares-Ruiz and S. T. Petcov, Nucl. Phys. **B712**, 392 (2005).
[13] C. H. Albright *et al.* (Neutrino Factory/Muon Collider Collaboration), arXiv:physics/0411123.
[14] A. Bandyopadhyay *et al.* (ISS Physics Working Group), arXiv:0710.4947.
[15] S. K. Agarwalla, S. Rakshit, and A. Raychaudhuri, Phys. Lett. B **647**, 380 (2007).
[16] R. Adhikari, S. K. Agarwalla, and A. Raychaudhuri, Phys. Lett. B **642**, 111 (2006).
[17] J. Kopp, M. Lindner, and T. Ota, Phys. Rev. D **76**, 013001 (2007).
[18] J. Kopp, M. Lindner, T. Ota, and J. Sato, Phys. Rev. D **77**, 013007 (2008).

[19] N. C. Ribeiro, H. Minakata, H. Nunokawa, S. Uchinami, and R. Zukanovich-Funchal, J. High Energy Phys. 12 (2007) 002.
[20] N. Cipriano Ribeiro, H. Nunokawa, T. Kajita, S. Nakayama, P. Ko, and H. Minakata, Phys. Rev. D **77**, 073007 (2008).
[21] P. Langacker and D. London, Phys. Rev. D **38**, 907 (1988).
[22] S. Antusch, C. Biggio, E. Fernandez-Martinez, M. B. Gavela, and J. Lopez-Pavon, J. High Energy Phys. 10 (2006) 084.
[23] A. Abada, C. Biggio, F. Bonnet, M. B. Gavela, and T. Hambye, J. High Energy Phys. 12 (2007) 061.
[24] P. Minkowski, Phys. Lett. B **67**, 421 (1977).
[25] T. Yanagida, in *Proceedings of the Workshop on the Unified Theory and the Baryon Number in the Universe*, edited by O. Sawada and A. Sugamoto (KEK, Tsukuba, Japan, 1979), p. 95.
[26] M. Gell-Mann, P. Ramond, and R. Slansky, *Supergravity*, edited by P. van Nieuwenhuizen and D. Z. Freedman (North Holland, Amsterdam, 1979), p 315.
[27] S. L. Glashow, *Proceedings of the 1979 Cargèse Summer Institute on Quarks and Leptons*, edited by M. Lévy, J.-L. Basdevant, D. Speiser, J. Weyers, R. Gastmans, and M. Jacob (Plenum Press, New York, 1980), p. 687.
[28] R. N. Mohapatra and G. Senjanovic, Phys. Rev. Lett. **44**, 912 (1980).
[29] J. Schechter and J. W. F. Valle, Phys. Rev. D **22**, 2227 (1980).
[30] J. Schechter and J. W. F. Valle, Phys. Rev. D **25**, 774 (1982).
[31] W. Buchmuller and C. Greub, Nucl. Phys. **B363**, 345 (1991).
[32] G. Ingelman and J. Rathsman, Z. Phys. C **60**, 243 (1993).
[33] J. Gluza, Acta Phys. Pol. B **33**, 1735 (2002).
[34] W. Loinaz, N. Okamura, S. Rayyan, T. Takeuchi, and L. C. R. Wijewardhana, Phys. Rev. D **68**, 073001 (2003).
[35] J. Kersten and A. Y. Smirnov, Phys. Rev. D **76**, 073005 (2007).
[36] S. Bray, J. S. Lee, and A. Pilaftsis, Nucl. Phys. **B786**, 95 (2007).
[37] F. del Aguila, J. A. Aguilar-Saavedra, and R. Pittau, J. High Energy Phys. 10 (2007) 047.
[38] A. Pilaftsis and T. E. J. Underwood, Nucl. Phys. **B692**, 303 (2004).
[39] A. Pilaftsis and T. E. J. Underwood, Phys. Rev. D **72**, 113001 (2005).
[40] Z. z. Xing and S. Zhou, Phys. Lett. B **653**, 278 (2007).
[41] R. N. Mohapatra and J. W. F. Valle, Phys. Rev. D **34**, 1642 (1986).
[42] E. Nardi, E. Roulet, and D. Tommasini, Phys. Lett. B **344**, 225 (1995).
[43] D. Tommasini, G. Barenboim, J. Bernabeu, and C. Jarlskog, Nucl. Phys. **B444**, 451 (1995).
[44] F. de Campos, O. J. P. Eboli, M. B. Magro, W. Porod, D. Restrepo, M. Hirsch, and J. W. F. Valle, J. High Energy Phys. 05 (2008) 048, and references contained in this.
[45] A. Gouvêa, G. F. Giudice, A. Strumia, and K. Tobe, Nucl. Phys. **B623**, 395 (2002).
[46] J. G. Korner, A. Pilaftsis, and K. Schilcher, Phys. Lett. B **300**, 381 (1993).
[47] J. Bernabeu, J. G. Korner, A. Pilaftsis, and K. Schilcher, Phys. Rev. Lett. **71**, 2695 (1993).
[48] C. P. Burgess, S. Godfrey, H. Konig, D. London, and I. Maksymyk, Phys. Rev. D **49**, 6115 (1994).
[49] G. Bhattacharya, P. Kalyniak, and I. Melo, Phys. Rev. D **51**, 3569 (1995).
[50] A. Ilakovac and A. Pilaftsis, Nucl. Phys. **B437**, 491 (1995).
[51] S. Bergmann and A. Kagan, Nucl. Phys. **B538**, 368 (1999).
[52] S. M. Bilenky and C. Giunti, Phys. Lett. B **300**, 137 (1993).
[53] M. Czakon, J. Gluza, and M. Zralek, Acta Phys. Pol. B **32**, 3735 (2001).
[54] F. del Aguila and M. Zralek, Acta Phys. Pol. B **33**, 2585 (2002).
[55] B. Bekman, J. Gluza, J. Holeczek, J. Syska, and M. Zralek, Phys. Rev. D **66**, 093004 (2002).
[56] J. Holeczek, J. Kisiel, J. Syska, and M. Zralek, Eur. Phys. J. C **52**, 905 (2007).
[57] E. Fernandez-Martinez, M. B. Gavela, J. Lopez-Pavon, and O. Yasuda, Phys. Lett. B **649**, 427 (2007).
[58] Z-z Xing, Phys. Lett. B **660**, 515 (2008).
[59] R. Acquafredda *et al.* (OPERA Collaboration), New J. Phys. **8**, 303 (2006).
[60] C. Vignoli, D. Barni, J. M. Disdier, D. Rampoldi, and G. Passardi (ICARUS Collaboration), in *Advances in Cryogenic Engineering*, AIP Conf. Proc. No. 823 (AIP, New York, 2006), p. 1643.
[61] A. Dighe and S. Ray, Phys. Rev. D **76**, 113001 (2007).
[62] E. K. Akhmedov, R. Johansson, M. Lindner, T. Ohlsson, and T. Schwetz, J. High Energy Phys. 04 (2004) 078.
[63] M. Honda, N. Okamura, and T. Takeuchi, arXiv:hep-ph/0603268.
[64] H. Nunokawa, S. Parke, and J. W. F. Valle, Prog. Part. Nucl. Phys. **60**, 338 (2008).
[65] D. Autiero *et al.*, Eur. Phys. J. C **33**, 243 (2004).
[66] P. Huber, M. Lindner, and W. Winter, Comput. Phys. Commun. **167**, 195 (2005).
[67] P. Huber, J. Kopp, M. Lindner, M. Rolinec, and W. Winter, Comput. Phys. Commun. **177**, 432 (2007).
[68] A. Badertscher, talk at NuFACT 06.
[69] C. Giunti, arXiv:hep-ph/0409230.